ORIGINAL PAPER

Structural elucidation of a Mn(III) derivative anchored with a tetradentate Schiff base precursor: in vitro cytotoxicity study

Kuheli Das[1] · Manasa G. Shetty[2] · Sindhoora K. Melanthota[2] · Babitha K. Sundara[2] · Sudeshna Kar[3] · Chiara Massera[4] · Eugenio Garribba[5] · Amitabha Datta[6] · Nirmal Mazumder[2]

Abstract

A new mononuclear Mn(III) derivative, $[Mn(L)(H_2O)_2]ClO_4$ (**1**) was obtained by reacting manganese perchlorate with the tetradentate Schiff base precursor, H_2L, [where $H_2L = C_6H_3(OMe)(OH)CH=N(CH_2)_3N=CH(OH)(OMe)C_6H_3$] and characterized by various spectral techniques. Single crystal X-ray diffraction analysis revealed that in 1, the central Mn atom is hexa-coordinated via the NNOO donor sites of the Schiff base precursor and two water molecules, yielding a distorted octahedral geometry. Also, the EPR spectra of **1** were recorded at the solid state by varying the temperature (from 90 to 300 K) as well as in different organic solvents; DMSO, MeOH and a mixture CH_2Cl_2/toluene; the results obtained agree with the geometrical environment around the metal. The cytotoxic activity of the Mn(III) derivative was evaluated against normal and cancer cell lines. The derivative exhibited comparatively better cytotoxic activity against MCF-7 cells compared to SiHa and fibroblast cells.

Kuheli Das and Manasa G. Shetty have contributed equally to this work.

✉ Nirmal Mazumder
nirmaluva@gmail.com

Amitabha Datta
amitd_ju@yahoo.co.in

[1] Department of Chemistry, University of Calcutta, 92 A.P.C. Road, Kolkata 700009, India

[2] Department of Biophysics, Manipal School of Life Sciences, Manipal Academy of Higher Education, Manipal 576104, Karnataka, India

[3] Department of Chemistry, School of Basic and Applied Science, Adamas University, Kolkata, India

[4] Dipartimento di Scienze Chimiche, della Vita e della Sostenibilità Ambientale, Università degli Studi di Parma, Viale delle Scienze 17/A, 43124 Parma, Italy

[5] Dipartimento di Medicina, Chirurgia e Farmacia, Università di Sassari, Viale San Pietro, 07100 Sassari, Italy

[6] Institute of Chemistry, Academia Sinica, Nankang, Taipei 115, Taiwan

Introduction

Because of their structural diversification, Schiff base-mediated metal derivatives are the indispensable stereo-chemical frameworks for coordination and organometallic chemistry (Rezaeivala and Keypour 2014; Low et al. 2016). The design of new multidentate precursors containing oxygen and nitrogen donors and of their corresponding metal derivatives has long attracted chemists due to their wide use in the discovery of new drugs, as well as catalytic and biological applications (Mahmoudabadi et al. 2019; Habibi et al. 2018; Keypour et al. 2017). Their ease of synthesis and reactivity with almost all metal ions present in the periodic table make them suitable synthons for the development of coordination chemistry. Furthermore, they form stabilized metal complexes with various oxidation states (Cozzi 2004; Köse et al. 2015; Ourari et al. 2014). Schiff base manganese complexes are efficient catalysts in biological chemistry because of their binding modes with O and N donor atoms (Luaces et al. 1996); they can be sterically and electronically modified to enhance their catalytic activity (Bagherzadeh et al. 2008; Ray et al. 2014; Ceyhan et al. 2012) by modifying the substituents on the aromatic ring. Due to the importance of Mn(III)

in diverse chemical and biological fields in recent years, research in connection with the organometallic chemistry of Mn(III) has been very active (Kirby et al. 1981; Christou 1989; Brudvig and Crabtree 1989; Vincent and Christou 1989; Wieghardt 1989; Que and True 1990). To obtain high-valent manganese(III) complexes, a high number of different ligating systems were probed to see if they could mimic the structural components of the active site; thus, the Schiff base precursors can participate as effective biometric ligands. Manganese(III) salen complexes [salen = N, N%-bis(salicylideneaminato)ethylene] have been previously reported (Chidara and Du 2013; Noritake et al. 2013; Rouco et al. 2020) and have been exploited in distinct areas such as catalysis (Routier et al. 1997; Muller et al. 1994; Puglisi et al. 2004), as simple models for active sites of metalloenzymes and proteins (Pecoraro 1992; Rousselot-Pailley et al. 2009), for mimicking the function of cytochrome p-450 and as models as well as for the treatment of ROS (reactive oxygen species)-associated disease including ischemic tissue damage (Park and Lim 2009; Bruce et al. 1996; Doctrow et al. 2002) and as molecular magnets (Bhargavi et al. 2009; Clérac et al. 2002). Fluorescence spectroscopy is a key tool for the qualitative and quantitative measurements of the fluorophores present in the compound. It helps in the identification of specific additives present in the sample. Moreover, fluorescence decay measurements provide information about the stability of the fluorophore in the excited state. Its intensity depends on the excitation wavelength, self-absorption by the sample and concentration of fluorophore (Lakowicz 2006).

In the current contribution, we describe the synthesis and crystallographic characterization of a new mononuclear Mn(III) system, [Mn(L)(H$_2$O)$_2$]ClO$_4$ (**1**) [where H$_2$L=CH$_2$[CH$_2$N=CH(C$_6$H$_3$OCH$_3$OH)]$_2$] (Thakurta et al. 2010) prepared in an aqueous methanolic medium. To characterize the complex, spectral studies (IR, UV–Vis, Emission, Fluorescence and EPR) were performed. The derivative was biologically evaluated against fibroblast (normal), SiHa (human cervical cancer) and MCF-7 (human breast cancer) cell lines.

Experimental

Materials

Mn(ClO$_4$)$_2$·6H$_2$O was acquired from Merck, India, whereas o-vanillin and 1,3-diaminopropane were purchased from Sigma-Aldrich. The reagent-grade solvents were used without further purification. The Schiff base precursor was synthesized according to the literature (Mani et al. 1994). All the reactions were carried out in aerobic conditions.

Physical measurements

A Perkin–Elmer 2400 CHNS/O elemental analyzer was used for recording the elemental analysis data (C, H, and N). The FTIR spectra were collected as KBr pellets on a Perkin–Elmer RX-1 spectrophotometer in the range 3550–450 cm^{-1}. UV–vis absorption spectra were acquired using a standard laboratory grade spectrophotometer (VarioskanTM LUX multimode microplate reader, Thermo Scientific, India). The fluorescence spectroscopy was performed using the same spectrophotometer, and the sample fluorescence was measured over a spectral range of 238–650 nm. The sample was prepared by dissolving 1 mg of the compound in 1 ml of dimethylsulfoxide (DMSO) and loaded in a corning flat bottom 96 well plate in triplicates for the fluorescence acquisition. The fluorescence spectra were analyzed and plotted using the OriginPro software. EPR spectra were recorded from 0 to 8000 Gauss in the temperature range 90–300 K with an X-band (9.4 GHz) Bruker EMX spectrometer equipped with an HP 53150A microwave frequency counter and a variable temperature unit. The microwave frequency was 9.40–9.41 GHz, microwave power was 20 mW (which is, with the ER4119 HS resonator, below the saturation limit), time constant was 81.92 ms, modulation frequency 100 kHz, modulation amplitude 0.4 mT, and resolution 8192 points.

Synthesis of the Schiff base ligand (H$_2$L)

1,3-Diaminopropane (10 mmol, 0.835 ml) and o-vanillin (20 mmol, 3.04 g) were refluxed in 50 ml of MeOH. The resulting mixture was cooled down and the excess solvent was removed under vacuum. A yellow-colored crystalline solid was obtained with a 73% yield.

Synthesis of compound 1

A 10 ml methanolic solution of the ligand (1 mmol) was added dropwise to a 1 ml methanolic solution of Mn(ClO$_4$)$_2$·6H$_2$O (0.361 g, 1 mmol) under constant stirring. The resulting mixture was boiled for ten minutes. After that, the brown-colored solution was kept undisturbed at room temperature. Dark brown, rectangular-shaped single crystals of **1** were generated after 1 week. The crystals were isolated very carefully by filtration and dried in air before carrying out the physical experiments. Yield: 0.58 g Anal. Calc. for C$_{19}$H$_{24}$O$_{10}$N$_2$MnCl: C, 42.95; H, 4.56; N, 5.28. Found: C, 42.68; H, 4.83; N, 5.47%.

X-ray crystallography

The crystal structure of compound 1 was determined by X-ray diffraction methods. Intensity data and cell parameters were recorded at 190(2) K on a Bruker ApexII diffractometer (MoKα radiation $\lambda = 0.71073$ Å) equipped with a CCD area detector and a graphite monochromator. The raw frame data were processed using the programs SAINT and SADABS to yield the reflection data files (AXS, SADABS Bruker, and Wisconsin Madison 1999). The structure was solved by direct methods using the SIR97 program (Altomare et al. 1999) and refined on F_o^2 by full-matrix least-squares procedures, using the SHELXL-2014/7 program (Sheldrick 2008) in the WinGX suite v.2014.1 (Farrugia 2012). The structure of the title compound was refined as a two-component inversion twin. All non-hydrogen atoms were refined with anisotropic atomic displacements, except for two disordered oxygen atoms of a perchlorate anion. The carbon-bound H atoms were placed in calculated positions and refined isotopically using a riding model with C–H ranging from 0.95 to 0.99 Å and Uiso(H) set to 1.2/1.5Ueq(C). The H atoms of the water molecules were found in the difference Fourier map and were subsequently refines setting the O–H distance to 0.87 Å with Uiso(H) = 1.5Ueq(O). The weighting scheme used in the last cycle of refinement was $w = 1/[\sigma^2 F_o^2 + (0.0772P)^2 + 0.6138P]$, where $P = (F_o^2 + 2F_c^2)/3$. Crystal data and experimental details for data collection and structure refinement are reported in Table 2.

Cell culture

Fibroblast (normal), human cervical cancer (SiHa) and human breast cancer (MCF-7) cell lines were obtained from ATCC, and cells were grown in Dulbecco's Modified Eagle Medium (DMEM), DMEM F12 (Himedia) supplemented with 10% FBS (Himedia). The stock solutions of 1 were prepared in dimethyl sulfoxide (DMSO) (Merck) and added at desired concentrations to the cell culture. All the cell lines were cultured at humidified atmosphere containing 5% CO_2 at 37 °C. The DMSO concentration did not exceed 0.1% in the final culture.

Cell viability assessment

Cancer and normal human cells were seeded at a density of 1.0×10^4 (SiHa and MCF-7) and 5.0×10^3 (fibroblast) cells per well, respectively, in a 96-well cell tissue culture plates with the medium supplemented with 10% FBS and the cells were allowed to attach for 24 h. The cells were then treated with various concentrations (0.1–100 μg/ml) of the compound. After 48 h of treatment, the cells were treated with 5 mg/ml 3-(4,5-dimethylthiazol-2-yl)-2,5-diphenyltetrazolium bromide (MTT) (Sigma) at 37 °C for

4 h. The media were removed after incubation, and DMSO (Merck) was added to each well to dissolve the formazan crystals. The absorbance at 570 nm and 630 nm of each well was measured using a microplate reader (VarioskanTM Thermo Scientific). The IC50 values of the compound in all the three cell lines were calculated using the Prism 8 software (GraphPad Software, CA). Experiments were conducted in triplicate (Mosmann 1983).

Results and discussion

Synthesis and characterization

The tetradentate Schiff base precursor, H_2L [where $H_2L = C_6H_3(OMe)(OH)CH=N(CH_2)_3N=CH(OH)(OMe)C_6H_3$] is a condensed product of *o*-vanillin and 1,3-diaminopropane in aerobic condition. The stoichiometric reaction of H_2L and $Mn(ClO_4)_2 \cdot 6H_2O$ in methanol afforded compound **1** with a 65% yield (see Scheme 1). The crystals were collected via vacuum filtration and washed with cold methanol.

The FTIR spectrum of **1** was carried out using KBr pallets in the 4000–400 cm^{-1} range and showed the key stretches diagnostic of the formation of the metal derivative. The vibration ν_{C-O} (phenolic) is responsible for the band observed at 1254 cm^{-1} for the free ligand (Nakamoto 2009); after complexation this band shifts at 1250 cm^{-1}. A band at 3450 cm^{-1} is observed for the free ligand due to the $\nu_{(O-H)}$ stretching frequency, but it disappears after complex formation. The stretching frequency $\nu_{C=N}$ for **1** appears in the lower region at 1611 cm^{-1}, indicating that the metal center is coordinated with the nitrogen atom (You and Zhu 2004), while the same band appears at 1643 cm^{-1} for the free ligand. The appearance of a corresponding band at 459 cm^{-1}, which is primarily due to the ν_{M-N} stretching frequency, supports ligand coordination to the metal center.

UV–Visible spectroscopy

In the range from ultraviolet to visible (200–800 nm), the absorption spectra were measured via synchronize scanning. The sample was dissolved in methanol. The free ligand shows maximum absorbance at 224, 264 and 415 nm with a weak shoulder at 292 nm. These are basically $\pi \rightarrow \pi^*$ and $n \rightarrow \pi^*$ transition bands. For the Mn-complex, it exhibits the electronic bands at 238 nm ($\varepsilon = 1.0 \times 10^4$ M^{-1} cm^{-1}) and 390 nm ($\varepsilon = 1.8 \times 10^3$ M^{-1} cm^{-1}) with a weak shoulder at 292 nm ($\varepsilon = 4.3 \times 10^3$ M^{-1} cm^{-1}). Absorbance values give similar extinction coefficients along with the λ_{max} found in previous experiments (Fronko et al. 1988; Lever 1984). Complex **1** exhibits a *d–d* band at 570 nm which reveals that Mn is in the oxidation state $+3$ in a hexa-coordinated
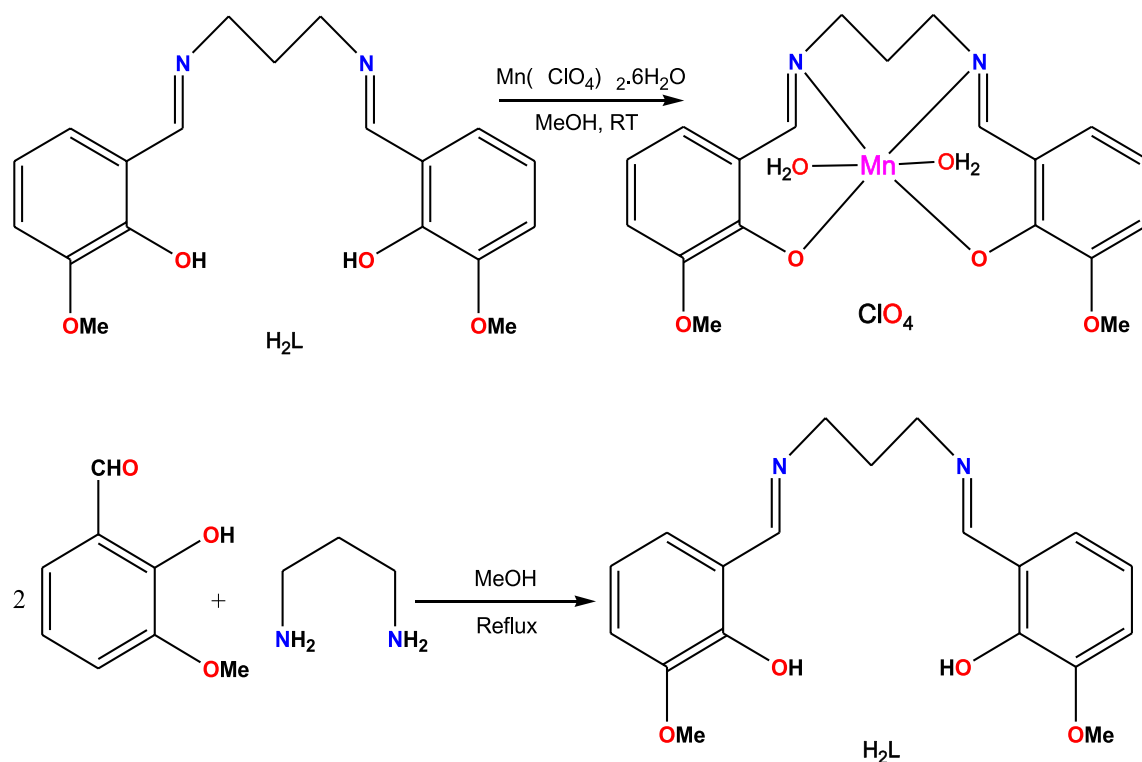
Scheme 1. The synthetic procedure of the Schiff base ligand

environment; indeed, Mn(II) does not show any *d–d* transition bands as high spin octahedral d^5 systems are spin forbidden.

Crystal structure

The crystal structure of 1 was elucidated through X-ray diffraction analysis on single crystals. It consists of a manganese complex of general formula [Mn(L)(H2O)2]ClO4, where H2L is the Schiff base CH2[CH2N=CH(C6H3OCH3OH)]2 comprising two OH groups. The complex crystallizes in the orthorhombic space group Pca21, with two independent complexes labeled A and B in the asymmetric unit. The two complexes show very similar geometrical parameters (see Fig. S1); the molecular structure of complex A is shown in Fig. 1.

[Mn(L)(H2O)2]ClO4 consists of a Mn(III) cation, one bideprotonated ligand L^{2-}, two water molecules and one perchlorate anion. The cation shows an octahedral geometry in which the equatorial plane is occupied by the tetradentate ligand through its two imine nitrogen atoms (N1A, N2A/N1B, N2B) and the two oxygen atoms of the phenoxy groups (O1A, O2A/O1B, O2B); the apical positions are occupied by two water molecules (O1WA, O2WA/O1WB, O2WB). Selected bond distances and angles for complexes A and B are reported in Table 1. The phenyl rings form two side

"wings" and are slightly inclined with respect to the equatorial plane of the octahedron (N1A–N2A–O1A–O2A and N1B–N2B–O1B–O2B). The angles formed between the mean planes are of 23.97(7)° for C6A–C10A, 29.49(9)° for C13A–C18A, 26.52(8)° for C6B–C10B and 23.70(7)° for C13B–C18B.

The main feature of the crystal structure is the formation of supramolecular chains along the *b*-axis direction in which molecules A and B alternate, connected by means of H-bonds involving the coordinated water molecules as donors and the Mn-bound oxygen anions as acceptors (as shown in Fig. 2 and Table 2). The perchlorate anions are placed between the parallel chains, forming C–H•••O interactions with the ligand.

Fluorescence spectroscopy

The sample fluorescence was measured at four different excitation wavelengths, specifically at 238 nm, 260 nm, 360 nm and 390 nm as shown in Fig. 3. The emission wavelength was set at a difference of 30 nm from the excitation wavelength, and the sample was scanned up to 650 nm with a step size of 2 nm. SkanIt Software 2.4.3 RE was used for the spectral acquisition with a measurement time of 100 ms. From the fluorescence spectrum, we observed multiple emission peaks as marked in Fig. 3.

Fig. 1 View of the molecular structure of [Mn(L)(H$_2$O)$_2$]ClO$_4$ with atom labeling scheme. The disorder from the perchlorate anion has been omitted for clarity
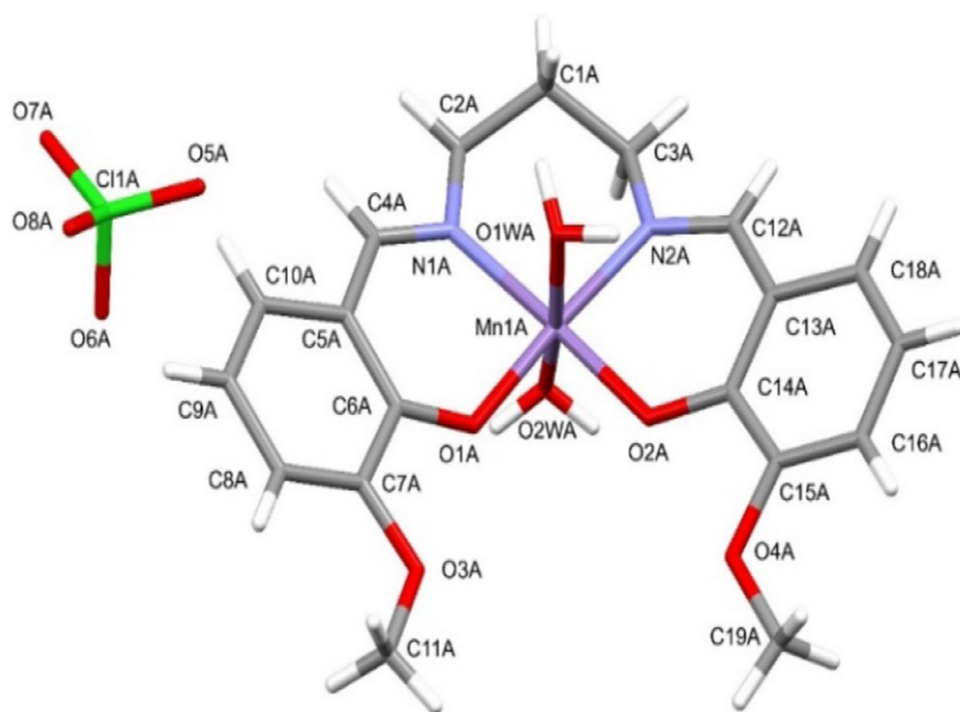
Table 1 Selected bond lengths [Å] and angles [°] for [Mn(L)(H$_2$O)$_2$]ClO$_4$

Mn1A–N1A	2.017(9)	Mn1B–N1B	2.013(8)
Mn1A–N2A	1.989(8)	Mn1B–N2B	2.063(7)
Mn1A–O1A	1.888(9)	Mn1B–O1B	1.896(8)
Mn1A–O2A	1.879(8)	Mn1B–O2B	1.905(9)
Mn1A–O1WA	2.229(9)	Mn1B–O1WB	2.180(8)
Mn1A–O2WA	2.189(8)	Mn1B–O2WB	2.185(7)
N1A–Mn1A–N2A	94.35(8)	N1B–Mn1B–N2B	94.75(8)
O1A–Mn1A–O2A	97.42(7)	O1B–Mn1B–O2B	87.02(6)
N1A–Mn1A–O1A	89.57(9)	N1B–Mn1B–O1B	89.16(7)
N2A–Mn1A–O2A	88.65(9)	N2B–Mn1B–O2B	89.06(9)
O1WA–Mn1A–O2WA	168.84(9)	O1WB–Mn1B–O2WB	167.63(8)

Moreover, the fluorescence decay of the sample was measured at the same excitation wavelengths with the emission set at their respective fluorescence maxima. The sample excited at 238 nm showed a longer lifetime, as shown in Fig. 3e.

The decay curve was fitted with a bi exponential curve using the OriginPro software as represented in Fig. 4. The equation underlying (Monisha et al. 2021; Das et al. 2017) the fit is given as follows.

$$I = A_1 e^{\left(\frac{-t1}{\tau_1}\right)} + A_2 e^{\left(\frac{-t2}{\tau_2}\right)}$$

where τ_1 and τ_2 are lifetime values, A_1 and A_2 represent amplitudes obtained from fitted curve, and $t1$ and $t2$ are time
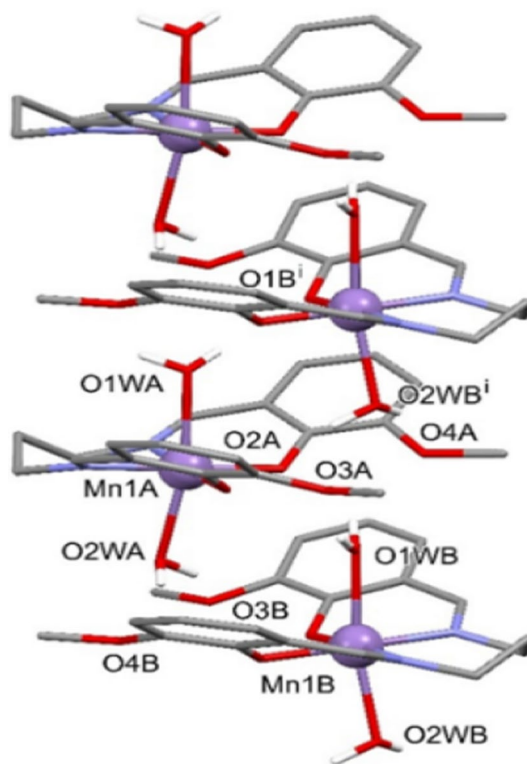
Fig. 2 View along the *b*-axis direction of the supramolecular chain formed by H-bonds involving the water molecules and the oxygen atoms of the ligand. Only the relevant H atoms are shown for clarity. Labeling scheme as in Table 2

Table 2 Relevant geometrical parameters (Å, °) for the hydrogen binding network in $[Mn(L)(H_2O)_2]ClO_4$

D–H⋯A	D–H	H⋯A	D⋯A	D–H⋯A
O1WB–H1WB⋯O3A	0.85	2.16	2.995(8)	165.8
O1WB–H2WB⋯O4A	0.85	2.77	2.985(9)	141.2
O1WB–H2WB⋯O2A	0.85	2.06	2.801(8)	144.5
O2WA–H3WA⋯O4B	0.87	1.89	2.698(7)	152.8
O2WA–H4WA⋯O3B	0.87	2.01	2.769(8)	144.5
O1WA–H2WA⋯O1B^i	0.87	2.08	2.737(8)	131.2
O2WB^i–H4WC^i⋯O4A	0.87	1.93	2.756(9)	158.5

$i = x, -1 + y, z$

constants. The overall lifetime of the compound is measured using the following relation, and it is found to be 69.34 μs.

$$\tau = \frac{A_1 \tau_1^2 + A_2 \tau_2^2}{A_1 \tau_1 + A_2 \tau_2}$$

The fluorescence emission of Mn-doped compound is observed at 385 nm, which supports the current study's findings (Tan et al. 2014). Furthermore, Randall's research demonstrates the fluorescence property of various Mn-based complexes (Randall 1939).
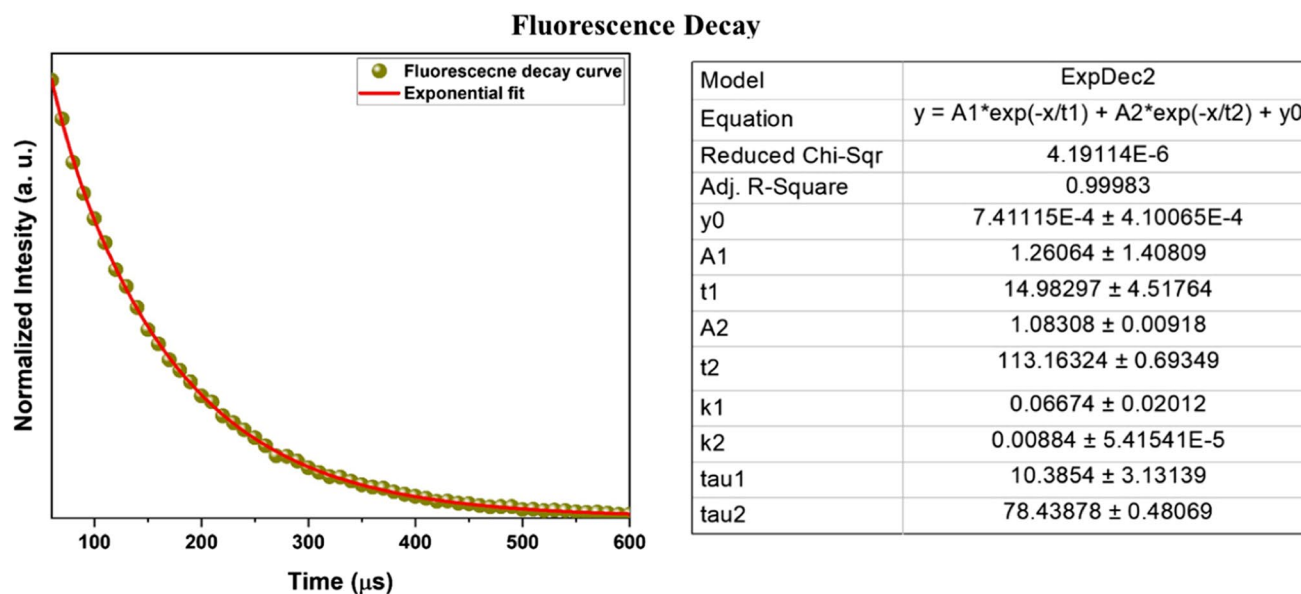
EPR spectroscopy

The EPR spectra on polycrystalline **1** were recorded in the solid state as a function of the temperature from 300 to 90 K (Fig. 5) and on the powder dissolved in an organic solvent like DMSO, MeOH and a mixture CH_2Cl_2/toluene 60/40 v/v (Fig. 6). All the spectra are EPR-silent and do not change with varying the temperature and the solvent, suggesting that the structure and oxidation state of **1** are maintained when varying the temperature and the organic solvent.

The lack of signals can be ascribed to the even number of electrons, to the large zero field splitting and fast relaxation time (Drago 1977; Mabbs and Collison 1992). These features indicate an oxidation state +3 for Mn, which is generally inactive at the X-band frequency (Carlin 1966);
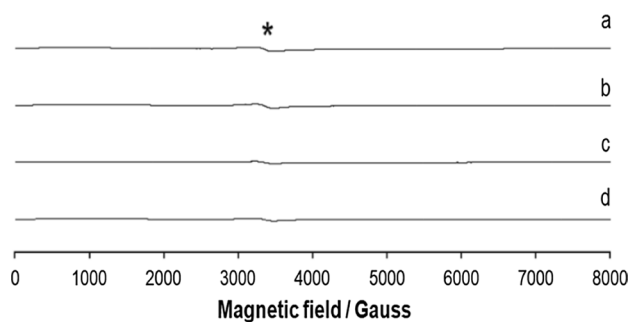
Fluorescence spectra
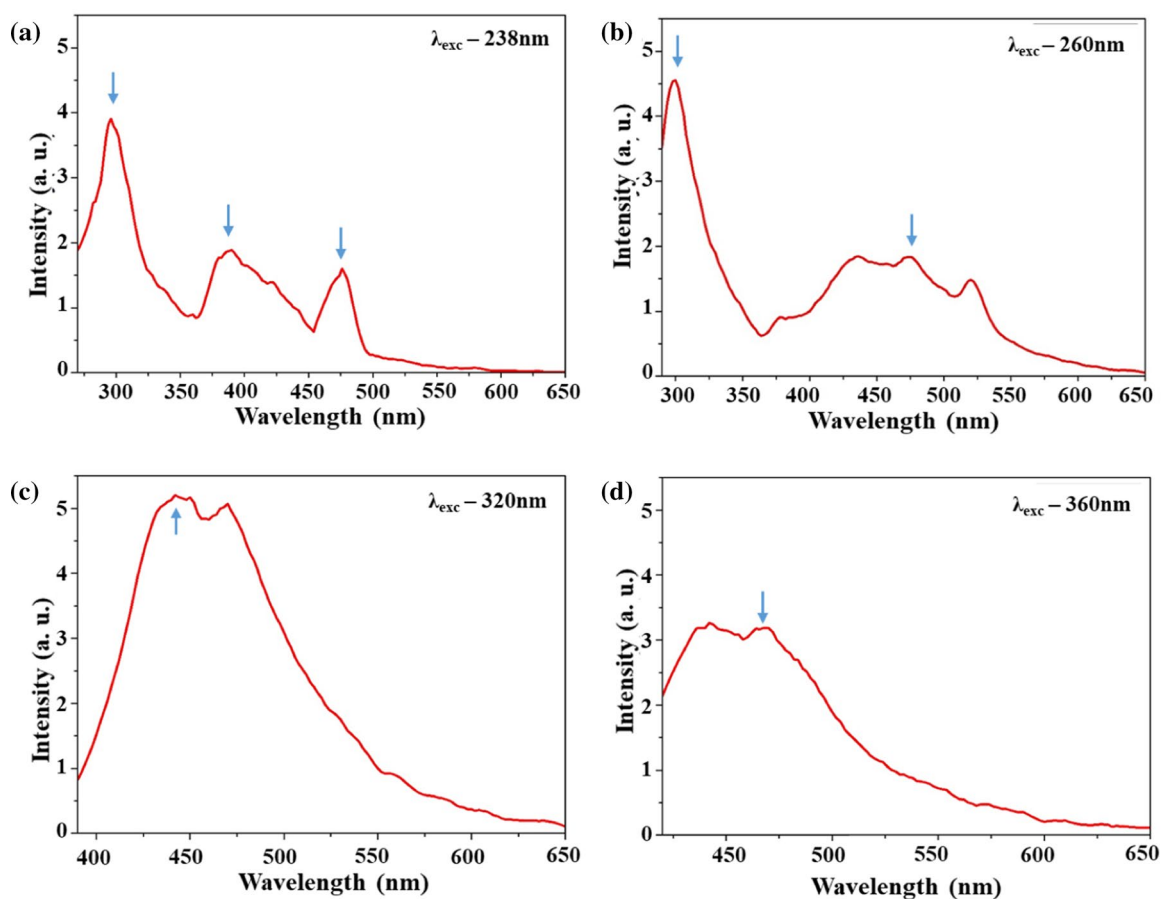
Fig. 3 Fluorescence measurements at, **a** 283 nm, **b** 260 nm, **c** 360 nm and **d** 390 nm excitation wavelengths

Fluorescence Decay

Model	ExpDec2
Equation	y = A1*exp(-x/t1) + A2*exp(-x/t2) + y0
Reduced Chi-Sqr	4.19114E-6
Adj. R-Square	0.99983
y0	7.41115E-4 ± 4.10065E-4
A1	1.26064 ± 1.40809
t1	14.98297 ± 4.51764
A2	1.08308 ± 0.00918
t2	113.16324 ± 0.69349
k1	0.06674 ± 0.02012
k2	0.00884 ± 5.41541E-5
tau1	10.3854 ± 3.13139
tau2	78.43878 ± 0.48069

Fig. 4 Fluorescence decay of the sample excited at 238 nm and emission recorded at 390 nm

Fig. 5 X-band EPR spectra of the complex **1** recorded as a function of the temperature at: **a** 300 K; **b** 180 K; **c** 130 K; **d** 90 K. With the asterisk the very weak resonances due to Mn(II) impurity are shown
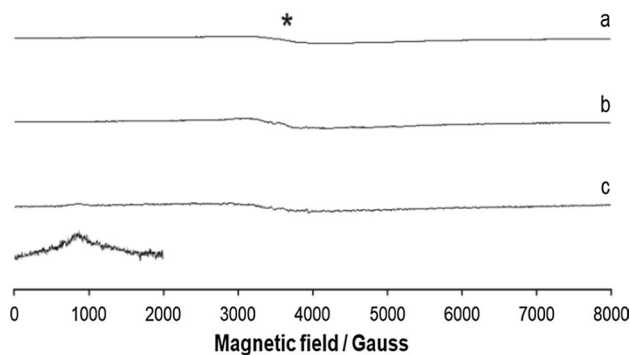

Fig. 6 X-band EPR spectra of complex **1** dissolved in: **a** CH_2Cl_2/toluene 60/40 v/v; **b** MeOH; **c** DMSO. The magnetic field range 0–2000 Gauss of the spectrum in DMSO was amplified 20 times. With the asterisk the weak resonances due to Mn(II) impurity are shown

on the contrary, Mn(II) (electronic configuration $3d^5$) and Mn(IV) (configuration $3d^3$) give a detectable spectrum even at room temperature. These findings are compatible with other Mn(III) complexes with a $S = 2$ spin state (Mani et al. 1994; Campbell et al., 2001; Syiemlieh et al. 2018). The very weak signal around $g = 2$ is assigned to Mn(II) ($S = 5/2$), often present as impurity in Mn(III) compounds (Bryliakov et al. 1999; Talsi and Bryliakov 2004). In DMSO an EPR signal at g value of ca 7.8 is detected. This resonance does not appear in MeOH or in the mixture CH_2Cl_2/toluene probably for the different solubility of the complex **1** in these solvents (Fig. 6). The absorption can be ascribed to the forbidden transition in the non-Kramers doublet, observed in Mn(III) and not in Mn(II) species (Bryliakov et al. 1999; Talsi and Bryliakov 2004; Dexheimer et al. 1989).

Magnetic susceptibility

To get an insight about the oxidation number and stereochemistry of the central metal ions in coordination frameworks, magnetic moments are often used in conjunction with electronic spectra. The spin and orbital angular momentum of its electrons are accountable for the magnetic properties of a complex. Nevertheless, in all cases, the spin-only magnetic moment persists, and the total numbers of unpaired electrons are correlated with it. The magnetic moment of complex 1 was calculated at room temperature, using the solid sample. The observed magnetic data ($\mu_{eff} = 4.92$ μ_B) are in good agreement with other Mn(III) derivatives in the literature (Dutta and Syamal 1982). Mn(III) is d^4 ($S = 2$) and
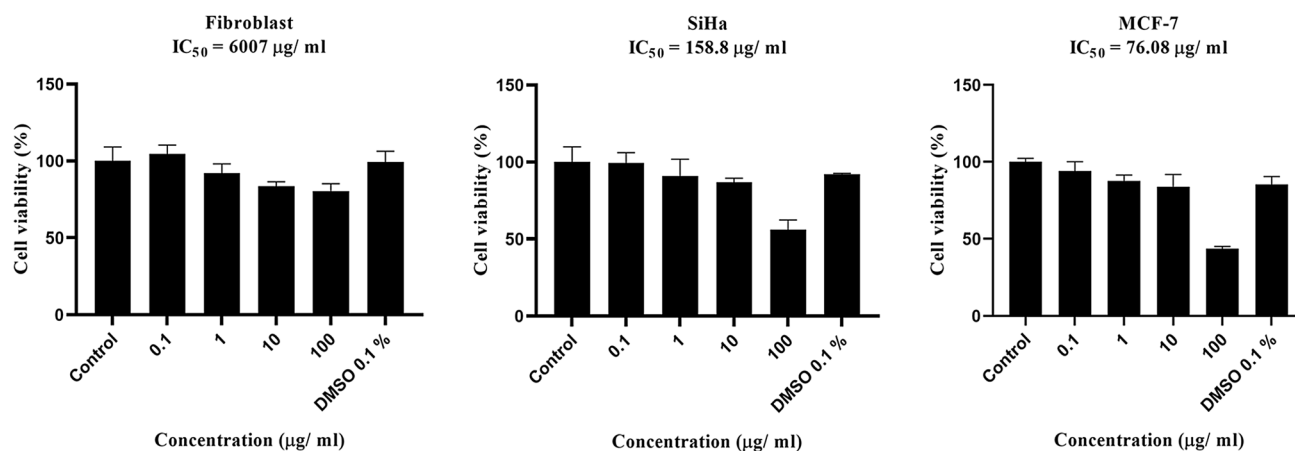
Fig. 7 Effects of the Mn(III) derivative on the survival of fibroblast, SiHa and MCF-7 cells with concentration ranging from 0.1 to 100 μg/ml by MTT assay after 48 h

given that both configurations exhibit unpaired electrons, it would be paramagnetic. Indeed, the magnetic studies evidence that complex 1 exhibits a high spin state, indicating that the energy gap between successive orbitals is low enough to allow electrons to occupy them; this results in a high spin atom with 4 unpaired electrons.

Cytotoxicity measurement

To assess the cytotoxic effects of the Mn(III) derivative on the survival of fibroblast, SiHA, and MCF-7 cell lines with concentration ranging from 0.1 to 100 μg/ml, a MTT assay was performed (Fig. 7). Cytotoxic effects were observed with an IC50 values of 6007 μg/ml (11,307 μM), 159 μg/ml (299 μM) and 76 μg/ml (143 μM) in fibroblast, SiHa and MCF-7 cells, respectively. The derivative exhibited potent cytotoxicity against the MCF-7 cell line when compared with SiHa. The cytotoxicity assay results indicated that the derivative is least cytotoxic to normal human cells, indicating that that Mn(III) complex causes a better cytotoxicity in human breast cancer cells, which agrees with previous research (Al-Anbaky et al. 2016).

Conclusions

We have reported a mononuclear Mn(III) derivative with a tetradentate Schiff base precursor, H_2L, [where $H_2L = C_6H_3(OMe)(OH)CH=N(CH_2)_3N=CH(OH)(OMe)C_6H_3$] which was characterized by several spectral techniques. The central Mn(III) atoms show a distorted octahedral environment confirmed by X-ray diffraction analysis. The fluorescence decay measured with 238 nm excitation and 390 nm emission shows a prominent decay pattern with lifetime of 69.34 μs and could be a powerful tool in practical

applications where the compound is used as the chemical sensor. The complex was evaluated for its cytotoxic activity against three different human cell lines (2 cancer cell lines and one normal cell line). Among the three cell lines, the derivative exhibited a better anti-proliferative activity against MCF-7 in comparison to SiHa. Also, it was least cytotoxic toward fibroblast cells. Further studies must be performed to synthesize new metal derivatives which could be good candidates for the biological process that involves the enzymatic breakdown of a cell's cytoplasm or cytoplasmic components.

Declarations

Conflict of interest On behalf of all authors, the corresponding author states that there is no conflict of interest.

References

Al-Anbaky Q, Al-Karakooly Z, Kilaparty SP, Agrawal M, Albkuri YM, RanguMagar AB, Ghosh A, Ali N (2016) Cytotoxicity of manganese(III) complex in human breast adenocarcinoma cell line is mediated by the generation of reactive oxygen species followed by mitochondrial damage. Int J Toxicol 35:672–682

Altomare A, Burla MC, Camalli M, Cascarano GL, Giacovazzo C, Guagliardi A, Moliterni AG, Polidori G, Spagna R (1999) SIR97: a new tool for crystal structure determination and refinement. J Appl Crystallogr 32:115–119. https://doi.org/10.1107/S0021889898007717

AXS, SADABS Bruker, and Wisconsin Madison (1999) USA, 2004; SAINT, Software Users Guide, Version 6.0; Bruker Analytical X-ray Systems. Software Users Guide, Version 6.0; Bruker Analytical X-ray Systems. Sheldrick, G. M. SADABS v2.03: Area-Detector Absorption Correction. University of Göttingen, Germany

Bagherzadeh M, Tahsini L, Latifi R (2008) Efficient oxidation of olefins and sulfides catalyzed by manganese(III)-tridentate Schiff base complex using UHP as oxidant. Catal Commun 9:1600–1606. https://doi.org/10.1016/j.catcom.2008.01.020

Bhargavi G, Rajasekharan MV, Costes JP, Tuchagues JP (2009) Synthesis, crystal structure and magnetic properties of dimeric MnIII Schiff base complexes including pseudohalide ligands: ferromagnetic interactions through phenoxo bridges and single molecule magnetism. Polyhedron 28:1253–1260. https://doi.org/10.1016/j.poly.2009.02.024

Bruce AJ, Malfroy B, Baudry M (1996) beta-Amyloid toxicity in organotypic hippocampal cultures: protection by EUK-8, a synthetic catalytic free radical scavenger. Proc Natl Acad Sci 93:2312–2316. https://doi.org/10.1073/pnas.93.6.2312

Brudvig GW, Crabtree RH (1989) Bioinorganic chemistry of manganese related to photosynthetic oxygen evolution. In: Stephen JL (ed) Progress in inorganic chemistry. Wiley, New York, pp 99–142

Bryliakov KP, Babushkin DE, Talsi EP (1999) Detection of EPR spectra in $S = 2$ states of MnIII (salen) complexes. Mendeleev Commun 9:29–32. https://doi.org/10.1070/MC1999v009n01ABEH001029

Campbell KA, Lashley MR, Wyatt JK, Nantz MH, Britt RD (2001) Dual-mode EPR study of Mn(III) salen and the Mn(III) salen-catalyzed epoxidation of cis-β-methylstyrene. J Am Chem Soc 123:5710–5719. https://doi.org/10.1021/ja0027463

Carlin RL (1966) Transition metal chemistry. Marcel Dekker, New York

Ceyhan G, Köse M, McKee V, Uruş S, Gölcü A, Tümer M (2012) Tetradentate Schiff base ligands and their complexes: synthesis, structural characterization, thermal, electrochemical and alkane oxidation. Acta Part A Mol Biomol Spectrosc 95:382–398. https://doi.org/10.1016/j.saa.2012.04.001

Chidara VK, Du G (2013) An efficient catalyst based on manganese salen for hydrosilylation of carbonyl compounds. Organometallics 32:5034–5037. https://doi.org/10.1021/om400805v

Christou G (1989) Manganese carboxylate chemistry and its biological relevance. Acc Chem Res 22:328–335. https://doi.org/10.1021/ar00165a006

Clérac R, Miyasaka H, Yamashita M, Coulon C (2002) Evidence for single-chain magnet behavior in a MnIII–NiII chain designed with high spin magnetic units: a route to high temperature metastable magnets. J Chem Soc 124:12837–12844. https://doi.org/10.1021/ja0203115

Cozzi PG (2004) Metal-Salen Schiff base complexes in catalysis: practical aspects. Chem Soc Rev 33:410–421. https://doi.org/10.1039/B307853C

Das K, Patra C, Sen C, Datta A, Massera C, Garribba E, El Fallah MS, Beyene BB, Hung CH, Sinha C, Askun T (2017) EPR interpretation, magnetism and biological study of a Cu(II) dinuclear complex assisted by a Schiff base precursor. J Biol Inorg Chem 22:481–495. https://doi.org/10.1007/s00775-016-1428-x

Dexheimer SL, Gohdes JW, Chan MK, Hagen KS, Armstrong WH, Klein MP (1989) Detection of EPR spectra in $S = 2$ states of trivalent manganese complexes. J Am Chem Soc 111:8923–8925. https://doi.org/10.1021/ja00206a028

Doctrow SR, Huffman K, Marcus CB, Tocco G, Malfroy E, Adinolfi CA, Kruk H, Baker K, Lazarowych N, Mascarenhas J, Malfroy B (2002) Salen−manganese complexes as catalytic scavengers of hydrogen peroxide and cytoprotective agents: structure—activity relationship studies. J Med Chem 45:4549–4558. https://doi.org/10.1021/jm020207y

Drago RS (1977) Physical methods in chemistry, 2nd edn. WB Saunders Company, Philadelphia

Dutta RL, Syamal A (1982) Elements of magnetochemistry, 2nd edn. S Chand & Company Ltd., New Delhi

Farrugia LJ (2012) WinGX and ORTEP for Windows: an update. J Appl Crystallogr 45:849–854. https://doi.org/10.1107/S0021889812029111

Fronko RM, Penner-Hahn JE, Bender CJ (1988) EPR spectral evidence for a dinuclear active site in the *Lactobacillus plantarum* manganese catalase. J Am Chem Soc 110:7554–7555. https://doi.org/10.1021/ja00230a055

Habibi D, Heydari S, Faraji A, Keypour H, Mahmoudabadi M (2018) A green and facile approach for the synthesis of N-monosubstituted ureas in water: Pd catalyzed reaction of arylcyanamides (an unexpected behavior of electron withdrawing groups). Polyhedron 151:520–529. https://doi.org/10.1016/j.poly.2018.05.049

Keypour H, Mahmoudabadi M, Shooshtari A, Bayat M, Ghassemzadeh M, Hosseinzadeh L, Mohsenzadeh F, Harms K (2017) Synthesis and characterization of two new N_4O_2 macrocyclic Schiff-base ligands containing piperazine moiety and mononuclear Co(III) and Cu(II) complexes, spectral, X-ray crystal structural, theoretical studies, cytotoxic and antibacterial properties. Polyhedron 129:189–198. https://doi.org/10.1016/j.poly.2017.03.035

Kirby JA, Robertson AS, Smith JP, Thompson AC, Cooper SR, Klein MP (1981) State of manganese in the photosynthetic apparatus. 1. Extended X-ray absorption fine structure studies on chloroplasts and di-. mu.-oxo-bridged dimanganese model compounds. J Am Chem Soc 103:5529–5537. https://doi.org/10.1021/ja00408a042

Köse M, Ceyhan G, Tümer M, Demirtaş İ, Gönül İ, McKee V (2015) Monodentate Schiff base ligands: their structural characterization, photoluminescence, anticancer, electrochemical and sensor properties. Acta Part A Mol Biomol Spectrosc 137:477–485. https://doi.org/10.1016/j.saa.2014.08.088

Lakowicz JR (2006) Principles of fluorescence spectroscopy. Springer, Boston

Low ML, Maigre L, Tahir MIM, Tiekink ER, Dorlet P, Guillot R, Ravoof TB, Rosli R, Pagès JM, Policar C, Delsuc N (2016) New

insight into the structural, electrochemical and biological aspects of macroacyclic Cu(II) complexes derived from S-substituted dithiocarbazate Schiff bases. Eur J Med Chem 120:1–12. https://doi.org/10.1016/j.ejmech.2016.04.027

Luaces L, Bermejo MR, Garcia-Vazquez JA, Romero J, Sousa A, Pritchard RG, McAuliffe CA, Mugnier Y (1996) Electrochemical synthesis of manganese(II) and (III) complexes derived from alicylaldehyde and 2-(2-aminoethyl) pyridine. Polyhedron 15:3717–3724. https://doi.org/10.1016/0277-5387(96)00120-9

Mabbs FE, Collison D (1992) Electron paramagnetic resonance of d transition metal compounds. Elsevier, Amsterdam

Mahmoudabadi M, Keypour H, Zebarjadian MH, Hosseinzadeh L (2019) Synthesis, cytotoxic activity, competitive ^{7}Li NMR studies of potentially N_6O_2 macroacyclic Schiff base ligands and corresponding manganese(II), zinc(II) and cadmium(II) complexes. Chem Data Collec 23:100263. https://doi.org/10.1016/j.cdc.2019.100263

Mani NS, Beall LS, Miller T, Anderson OP, Hope H, Parkin SR, Williams DJ, Barrett AGM, Hoffman BM (1994) Synthesis and characterisation of porphyrazinoctamine derivatives: X-ray crystallographic studies of [2, 3, 7, 8, 12, 13, 17, 18-octakis (dibenzylamino)-porphyrazinato] magnesium(II) and {2, 3, 7, 8, 12, 13, 17, 18-octakis [allyl (benzyl) amino]-porphyrazinato} nickel (II). J Chem Soc Chem Commun 18:2095–2096. https://doi.org/10.1039/C39940002095

Monisha M, Hegde V, Melanthota SK, Mazumder N, Sayyed MI, Al-Ghamdi H, Almuqrin AH, Kamath SD (2021) Photoluminescence studies on dysprosium doped glass ceramics containing α-Na$_3$AlF$_6$ crystalline phase for white light emission. Mat Chem Phys 274:125157

Mosmann T (1983) Rapid colorimetric assay for cellular growth and survival: application to proliferation and cytotoxicity assays. J Immun Methods 65:55–63. https://doi.org/10.1016/0022-1759(83)90303-4

Muller JG, Paikoff SJ, Rokita SE, Burrows CJ (1994) DNA modification promoted by water-soluble nickel(II) salen complexes: a switch to DNA alkylation. J Inorg Biochem 54:199–206. https://doi.org/10.1016/0162-0134(94)80013-8

Nakamoto K (2009) Infrared and Raman spectra of inorganic and coordination compounds, part B: applications in coordination, organometallic, and bioinorganic chemistry, 6th edn. Wiley, Hoboken

Noritake Y, Umezawa N, Kato N, Higuchi T (2013) Manganese salen complexes with acid–base catalytic auxiliary: functional mimetics of catalase. Inorg Chem 52:3653–3662. https://doi.org/10.1021/ic302101c

Ourari A, Ouennoughi Y, Aggoun D, Mubarak MS, Pasciak EM, Peters DG (2014) Synthesis, characterization, and electrochemical study of a new tetradentate nickel(II)-Schiff base complex derived from ethylenediamine and 5′-(N-methyl-N-phenylaminomethyl)-2′-hydroxyacetophenone. Polyhedron 67:59–64. https://doi.org/10.1016/j.poly.2013.08.056

Park W, Lim D (2009) Effect of the oligo (ethylene glycol) group on the antioxidant activity of manganese salen complexes. Bioorg Med Chem Lett 19:614–617. https://doi.org/10.1016/j.bmcl.2008.12.063

Pecoraro VL (1992) Manganese redox enzymes. Wiley, Weinheim

Puglisi A, Tabbì G, Vecchio G (2004) Bioconjugates of cyclodextrins of manganese salen-type ligand with superoxide dismutase activity. J Inorg Biochem 98:969–976. https://doi.org/10.1016/j.jinorgbio.2004.02.012

Que L Jr, True AE (1990) Dinuclear iron- and manganese-oxo centers in biology. In: Stephen JL (ed) Progress in inorganic chemistry: bioinorganic chemistry. Wiley, New York, pp 97–200

Randall JT (1939) The fluorescence of compounds containing manganese. Proc R Soc A Math Phys Eng Sci 170:272–293. https://doi.org/10.1098/rspa.1939.0032

Ray S, Konar S, Jana A, Das K, Dhara A, Chatterjee S, Kar SK (2014) Syntheses, crystal structure, spectroscopic and photoluminescence studies of mononuclear copper(II), manganese(II), cadmium(II), and a 1D polymeric Cu(II) complexes with a pyrimidine derived Schiff base ligand. J Mol Struct 1058:213–220. https://doi.org/10.1016/j.molstruc.2013.11.004

Rezaeivala M, Keypour H (2014) Schiff base and non-Schiff base macrocyclic ligands and complexes incorporating the pyridine moiety–the first 50 years. Coord Chem Rev 280:203–253. https://doi.org/10.1016/j.ccr.2014.06.007

Rouco L, Liberato A, Fernández-Trujillo MJ, Manez A, Basallote MG, Alvariño R, Alfonso A, Botana LM, Maneiro M (2020) Salen-manganese complexes for controlling ROS damage: neuroprotective effects, antioxidant activity and kinetic studies. J Inorg Biochem 203:110918. https://doi.org/10.1016/j.jinorgbio.2019.110918

Rousselot-Pailley P, Bochot C, Marchi-Delapierre C, Jorge-Robin A, Martin L, Fontecilla-Camps JC, Cavazza C, Ménage S (2009) The protein environment drives selectivity for sulfide oxidation by an artificial metalloenzyme. Chem Bio Chem 10:545–552. https://doi.org/10.1002/cbic.200800595

Routier SB, Bernier JL, Catteau MP, Bailly C (1997) Highly preferential cleavage of unpaired guanines in DNA by a functionalized salen-nickel complex. Bioorg Med Chem Lett 7:63–66. https://doi.org/10.1016/S0960-894X(96)00569-0

Seddon KR (1985) Inorganic electronic spectroscopy. In: Lever ABP (ed) Studies in physical and theoretical chemistry, 2nd edn. Elsevier, Amsterdam

Sheldrick GM (2008) A short history of SHELX. Acta Crystallogr Sect A 64:112–122. https://doi.org/10.1107/S0108767307043930

Syiemlieh I, Kumar A, Kurbah SD, De AK, Lal RA (2018) Low-spin manganese(II) and high-spin manganese(III) complexes derived from disalicylaldehyde oxaloyldihydrazone: synthesis, spectral characterization and electrochemical studies. J Mol Struct 1151:343–352. https://doi.org/10.1016/j.molstruc.2017.09.052

Talsi EP, Bryliakov KP (2004) X-band perpendicular-mode EPR spectra of EPR-silent manganese(III) porphyrins. Mendeleev Commun 14:111–112. https://doi.org/10.1070/MC2004v014n03ABEH001893

Tan TL, Lai CW, Abd Hamid SB (2014) Tunable band gap energy of Mn-doped ZnO nanoparticles using the coprecipitation technique. J Nanomater. https://doi.org/10.1155/2014/371720

Thakurta S, Butcher RJ, Gómez-García CJ, Garribba E, Mitra S (2010) Synthesis, structural aspects and magnetic properties of an unusual 2D thiocyanato-bridged cobalt(II)–Schiff base network. Inorg Chim Acta 363:3981–3986. https://doi.org/10.1016/j.ica.2010.07.069

Vincent JB, Christou G (1989) Higher oxidation state manganese biomolecules. Adv Inorg Chem 33:197–257. https://doi.org/10.1016/S0898-8838(08)60196-8

Wieghardt K (1989) The active sites in manganese-containing metalloproteins and inorganic model complexes. Angew Chem Int Ed Engl 28:1153–1172. https://doi.org/10.1002/anie.198911531

You ZL, Zhu HL (2004) Syntheses, crystal structures, and antibacterial activities of four Schiff base complexes of copper and zinc. Anorg Allg Chem 630:2754–2760. https://doi.org/10.1002/zaac.200400270